Journal of Computer Assisted Tomography
10(5):715–722, September/October

Blood Flow Imaging by Cine Magnetic Resonance

G. L. Nayler, D. N. Firmin, and D. B. Longmore

Abstract: A technique for measuring blood flow by whole body nuclear magnetic resonance is described. This method uses imaging gradient profiles that combine even echo rephasing with a field echo sequence to overcome the problem of signal loss from flowing blood. The flow velocity component in any desired direction may be measured by appropriate gradient profile modifications, producing velocity dependent phase shifts that can be displayed by phase mapping. The sequence allows for fast repetition so that flow information may be acquired rapidly from many points in the cardiac cycle and has been used in this mode to observe and measure blood flow in the heart chambers and great vessels. Flow measurements in the femoral artery were also carried out using the same technique; these were compared with similar measurements obtained by Doppler ultrasound. The technique can readily be applied using standard imaging equipment and should prove useful in the clinical assessment of many diseases of the cardiovascular system. **Index Terms:** Blood, flow dynamics—Heart, blood flow—Magnetic resonance imaging.

To date, several techniques have been described for the measurement of blood flow by magnetic resonance (MR) (1–11); some of these have used time-of-flight phenomena and others phase mapping. The time-of-flight techniques have proved difficult to quantify because they rely on signal amplitude measurement, which is dependent not only on the flow velocity but also on the proton density, T1, T2, and particularly on the type of flow (laminar, turbulent, constant, or pulsatile). Phase mapping techniques, on the other hand, look only at the pixel phases of images obtained using sequences designed to give phase shifts that are directly related to the flow velocity (4). This concentration on phase rather than intensity overcomes the difficulties encountered with variable pixel amplitudes in the time of flight methods.

One major problem that has greatly restricted the use of these techniques is the loss of signal that occurs from flowing blood. Although this loss is useful in cardiac and vascular imaging, since it provides contrast between blood and tissue and so helps to define anatomy, the fact remains that, without blood signal, blood flow cannot be measured. The signal loss is attributable to phase shifts caused by spins flowing along imaging gradients. If a particular arrangement of gradients is used, such as those in the read profile of the Carr-Purcell sequence, the phase coherence can be regained resulting in a higher signal. It has been found that this rephasing occurs for constant flow whenever an even numbered echo is formed with the gradients (12). This effect has also been analysed and illustrated in imaging terms by Waluch and Bradley (13) where they showed the signal intensity from blood in the hepatic vein was greater on the second echo image than the first.

Accelerating (nonconstant) flow has a similar dephasing effect on the second echo signal; it is for this reason that little signal is seen from the pulsatile flowing blood in arteries or in situations where turbulence is occurring. The technique described below uses the same even echo rephasing principle but with a much shorter echo time to avoid the signal loss. The basis of this work involves an interesting paradox: To measure flow, a sequence that was insensitive to flow had first to be designed. To accomplish this a specially designed field echo sequence, which could be made to give flow-dependent phase shifts in any of the three principal gradient directions, was used. The field echo sequence

From the Advanced Development Group, Picker International Ltd., East Lane Wembley, Middlesex (G. L. Nayler), and Magnetic Resonance Unit, National Heart and Chest Hospitals, Chelsea, London (D. N. Firmin and D. B. Longmore), England. Address correspondence and reprint requests to G. L. Nayler at Advanced Development Group, Picker International Ltd., Post Office Box 2, East Lane Wembley, Middlesex HA9 7PR, England.

has a further advantage in that it may be repeated rapidly with little signal loss from the blood. This allows us to make phase map flow measurements at numerous points of the heart cycle in the course of a single experiment, so reducing the time required to complete a full study.

THEORY

Flow Related Phase Shifts

From the early days of nuclear MR (NMR), it has been recognised that spin echoes resulting from magnetisation moving along a magnetic field gradient experience phase shifts dependent on the motion of the resonant material (14). The phase shift introduced to magnetisation subjected to a time varying magnetic field gradient is given by:

$$\phi = \int \gamma G(t)x(t)dt \qquad (1)$$

where ϕ is the phase shift, γ the magnetogyric ratio, $G(t)$ the gradient amplitude at time t, and $x(t)$ is the position of the magnetisation at time t.

Magnetisation undergoing a general motion may be described as the summation of a series of time derivatives of its position at a given point in time:

$$x(t) = x(0) + x'(0)t + \frac{x''(0)t^2}{2!} + \ldots + \frac{x^{[n]}(0)t^n}{n!} + \ldots \qquad (2)$$

or

$$x(t) = x(0) + \sum_{n=1}^{\infty} \frac{x^{[n]}(0)t^n}{n!} \qquad (3)$$

If terms higher than $n = 1$ are neglected for the magnetisation undergoing general motion, Eq. 1 becomes

$$\phi = x(0) \int \gamma G(t)dt + x'(0) \int \gamma G(t)tdt \qquad (4)$$

For the case of a modulated gradient (Fig. 1)

$$\int \gamma G(t)dt = 0 \qquad (5)$$

However

$$\int \gamma G(t)tdt \neq 0 \qquad (6)$$

so that a phase shift will be introduced due to the first order derivative of $x(0)$ the velocity. The magnitude of this phase shift is given by

$$\phi = \gamma G\delta\Delta v \qquad (7)$$

where G, δ, and Δ are the amplitude, duration, and separation, respectively, of the two gradient sections and v is the velocity of the imaged material.

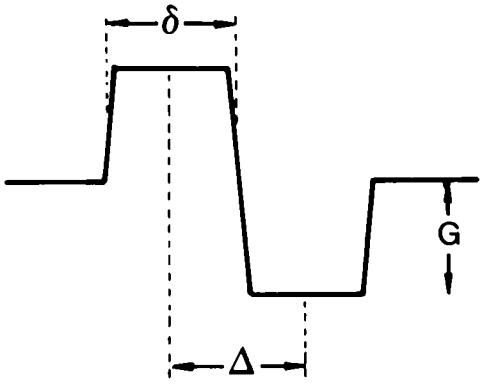

FIG. 1. A dipolar gradient modulation. δ, Δ, and G are the duration, separation, and amplitude of the two gradient sections, respectively.

Signal Loss

Flow related phase shifts such as those described above can result in loss of signal from the flowing material in two ways. First, the situation may arise where a single voxel contains material with a distribution of flow velocities. It follows that the net signal from this voxel will be made up of individual signals with a whole range of phases, this resulting in a proportion of phase cancellation and hence signal loss. As an example, laminar flow in the read gradient direction of a section of vessel completely enclosed within a voxel (Fig. 2a) is analysed below.

The flow profile is parabolic and described by

$$v(r) = v_{max}\left(1 - \frac{r^2}{a^2}\right) \qquad (8)$$

where v_{max} is the maximum velocity at the centre of the vessel, $v(r)$ is the velocity at a radius r from the centre, and a is the radius of the vessel.

The total signal is obtained by summation of all the signals dS from volume elements dV within the enclosed vessel. These have equal intensity given by the relaxation weighted spin density ρ but have a phase proportional to the local velocity, related by a proportionality constant k so that

$$dS = \rho \exp[ikv(r)]dV \qquad (9)$$

By integrating over the area of the vessel we get an expression for the signal intensity S

$$S = \int dr \int d\theta r\rho \exp\left[ikv_{max}\left(1 - \frac{r^2}{a^2}\right)\right] \qquad (10)$$

By normalising this to the corresponding signal intensity from stationary blood, the total signal is expressed in relative terms as

$$S_R = \frac{i}{kv_{max}}[1 - \exp(ikv_{max})] \qquad (11)$$

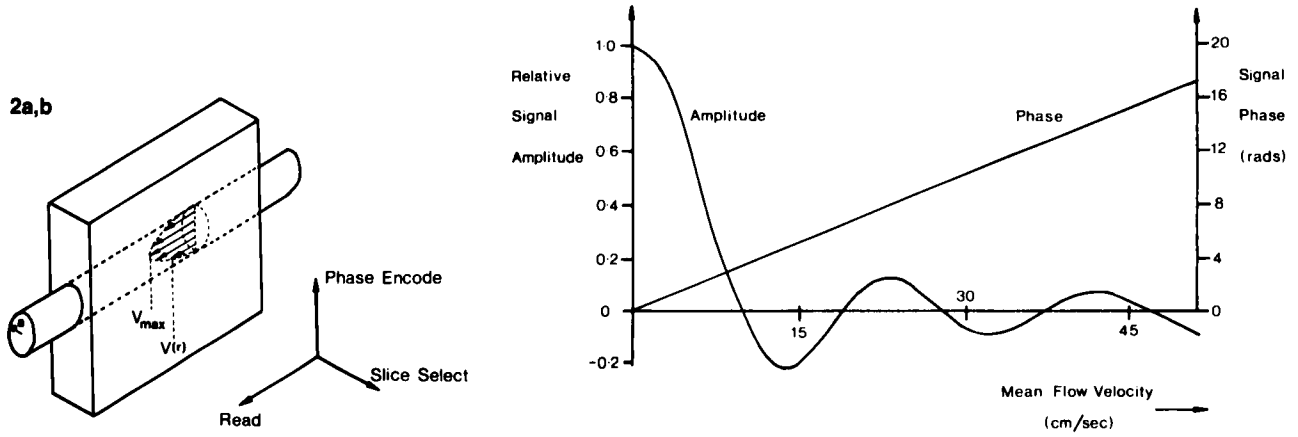

FIG. 2. a: Laminar flow, in the direction of the read gradient, down a section of tube completely enclosed in a single voxel. **b:** Relative signal amplitude and overall signal phase shift plotted against the mean flow velocity for the situation illustrated in (a) when a typical read gradient is used.

Figure 2b plots the amplitude of this relative signal as a function of the mean flow velocity for the case of a typical imaging read gradient. It may be seen that the relative signal amplitude rapidly reduces to <25% for velocities >7 cm/s.

The case of in vivo blood flow measurement is, however, considerably more complex than this simple model; blood is non-Newtonian and the flow profile depends on the time in the heart cycle and the particular vessel in question. A full attempt at calculating the signal loss in such a case must consider these additional factors; the principal conclusion of the simple model, that significant signal loss prises from the phase cancellation within a voxel at physiologically realistic flow velocities, does still apply, however.

The second source of signal loss results from the shift in phase of the overall signal arising from a voxel containing flowing material; this phase shift for the case of laminar flow described previously is also shown in Fig. 2b. It can be seen that the phase shift increases linearly with flow velocity, thus adding an extra term to the phase encoding process. This has no effect on the spatial localisation of the signal by the two-dimensional Fourier transform reconstruction as long as the velocity (and hence the phase shift term) stays constant from view to view. However, when blood flow in the body is considered, physiological factors that alter the duration of the heart cycle affect in turn the flow velocities on successive heart beats; the ensuing phase shifts result in any remaining signal intensity from the blood being spread out as artifact along the phase encoding dimension of the image.

Even Echo Rephasing

It may be seen that, if the gradient sequence of Fig. 1 and Eq. 7 is repeated but with all gradients applied in the opposite sense (Fig. 3a), the resultant phase shift will equal zero

$$\phi = \gamma G \delta \Delta v + \gamma(-G)\delta \Delta v = 0 \qquad (12)$$

So far only static and first-order motions have been

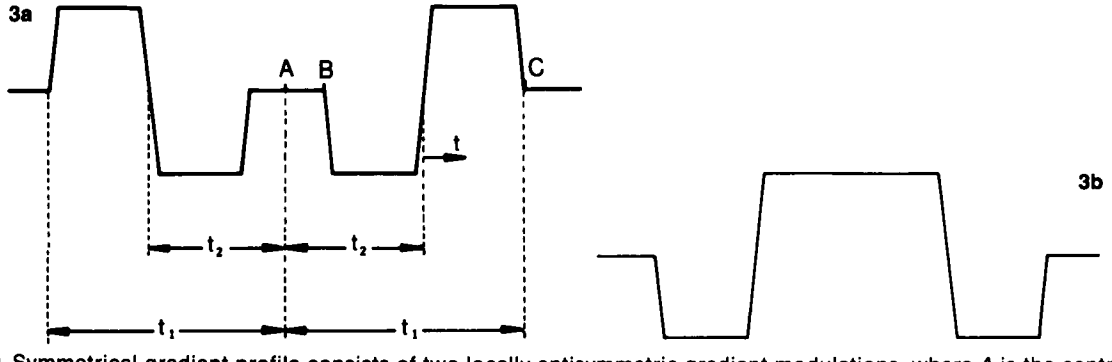

FIG. 3 a: Symmetrical gradient profile consists of two locally antisymmetric gradient modulations, where *A* is the centre of the profile, *B* and *C* are the beginning and end of the second gradient modulation, and t_1 and t_2 are the times from *A* to the limits of the profile and the centres of each modulated profile, respectively. **b:** An analogous profile with t_2 minimised by gradient pulse amalgamation.

considered; to examine the effect of higher order motions it is useful to consider times with respect to A, the centre of the profile (Fig. 3a).

By combining Eqs. 1 and 3, the phase shift over the duration of the gradient profile can be obtained:

$$\phi = \sum_{n=0}^{\infty} \frac{x^{[n]}(A)}{n!} \int_{A-t_1}^{A+t_1} \gamma G(t) t^n dt \qquad (13)$$

As the integral is taken over equal ranges to positive and negative times it vanishes when the integrand is an odd function of time. Therefore if the gradient is an even function of time (as in Fig. 3a) the phase shift of Eq. 13 will contain no contributions from odd derivatives of position. However, even derivatives (including acceleration) will remain, introducing phase shifts and thus causing signal loss. When, as in this case, each gradient modulation is locally antisymmetric the phase shift introduced by the higher order derivatives for the symmetrical gradient profile is given by

$$\phi = \sum_{n=0}^{\infty} 2x^{[2n]}(A) \sum_{j=1}^{n} \frac{t_2^{(2j-1)}}{(2j-1)!(2n-2j+1)!} \int_B^C \gamma G(t) t^{(2n-2j+1)} dt \qquad (14)$$

It should be noted that the expression only contains even differentials of position each multiplied by the time (t_2) between the centre of the complete profile (A) and the centre of each modulated gradient. To reduce the effect of the higher order differentials, therefore, this time should be minimised, e.g. as shown in Fig. 3b.

The NMR response of most moving systems may be analysed in the expansion form of Eq. 14. The accuracy with which the first few terms approximate to the true result, however, depends on the type of flow being considered. Essentially smooth pulsatile flow is thought to be accurately described by the first three to four differentials of position. In highly turbulent flow this limited approximation breaks down and more terms are required to describe the system adequately. In the extreme case of diffusion (microscopic flow) the approximation breaks down entirely, diffusive flow being an essentially random process better handled by probabilistic methods.

Sequence

The sequence used is illustrated in Fig. 4 and relies on symmetrical slice select and read gradient profiles that produce even echo rephasing. The phase encoding profile, which has a minor effect on the signal, is left unaltered. To encode flow information into the signal, the gradient profiles are modified and the required modifications, in each of the three directions, are shown by the dashed sections in Fig. 4. These involve simple time shifts of a portion of the gradient profile for the slice select

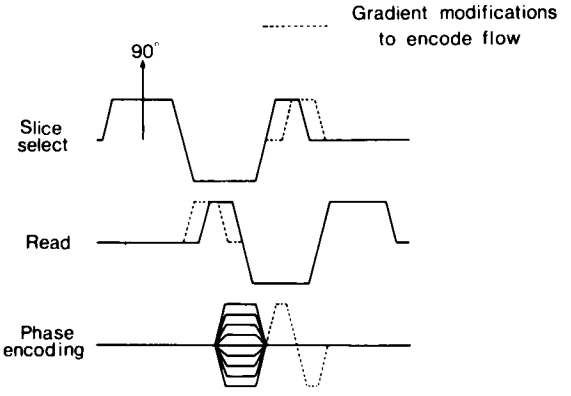

FIG. 4. The field even echo rephasing sequence. The modifications required to encode flow information (see text) are shown as dashed lines.

and read directions and a gradient modulation, as proposed by Moran (15), for the phase encode direction. When the gradient section is time shifted, the resultant phase difference as a function of velocity is given by

$$\phi = v\Delta \int \gamma G(t) dt \qquad (15)$$

where the integral is taken over the gradient pulse and Δ is the shift in time. The same relationship applies when a dipolar gradient modulation is introduced, in which case the integral is taken over only one gradient pulse and Δ is the separation between the centres of the two pulses.

Although the field echo sequence was primarily used to reduce the echo time, it was found to have a secondary advantage in that it could be repeated more rapidly than the spin echo sequence. The single 180° pulse in the spin echo sequence has the effect of partially saturating the magnetisation of blood outside the slice, resulting in very low signal when this blood flows into the imaging plane. One solution to this problem is to use a slice selected 180° pulse in the spin echo sequence. However, signal is lost at high flow velocities due to the flow of excited blood out of the slice between the 90 and

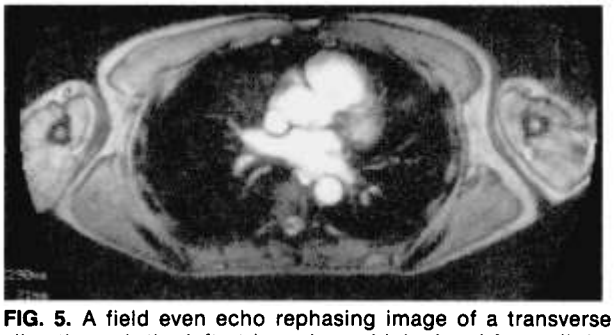

FIG. 5. A field even echo rephasing image of a transverse slice through the left atrium shows high signal from all the principal blood vessels in the slice.

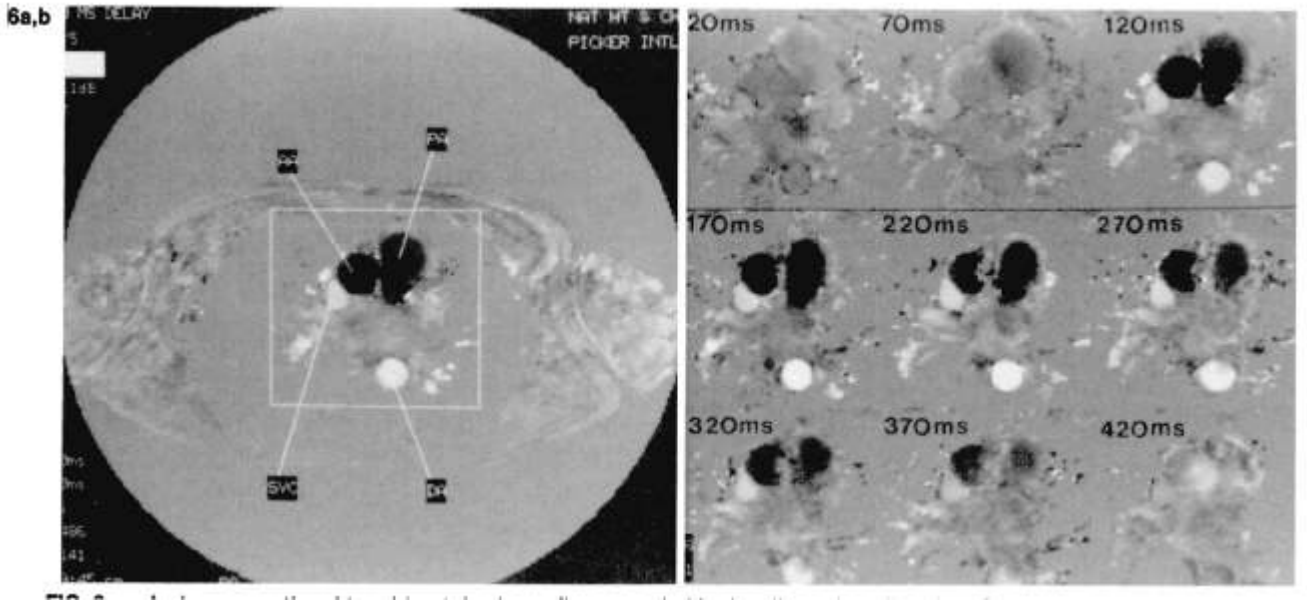

FIG. 6. a: A phase map timed to midsystole shows flow encoded in the slice select direction. Static material is midgrey, flow up the body tends towards black, and flow down towards white. Flow can be seen in the ascending aorta (AA), descending aorta (DA), pulmonary artery (PA), and the superior vena cava (SVC). The boxed area is the area of interest used in (b). **b:** Phase maps at R-wave delays from 20 to 420 ms, in 50 ms intervals show the variations in flow throughout the first half of the heart cycle.

180° pulses. The field echo sequence, having no 180° pulses, is not affected in this way. Saturation of blood within the slice is avoided by the use of a flip angle <90°. For stationary material the optimum angle may be calculated from the Ernst equation:

$$\text{angle} = \cos^{-1}[\exp(-TR/T1)] \qquad (16)$$

This does not apply exactly to flowing blood, however, the maximum signal being obtained at slightly higher flip angles, as the signal is enhanced by the flow of fully magnetised blood into the slice between excitations. Experimentally the optimum flip angle was found to be ~60°; the sequence could then be repeated as frequently as once every 50 ms without serious loss of signal from the blood and with partial saturation of the (largely) stationary cardiac tissue.

MATERIALS AND METHODS

These studies were carried out at the National Heart and Chest Hospital's MR unit using a Picker International 0.5 T system in conjunction with the sequence described above. The images were reconstructed on a 256 × 256 matrix, acquiring 128 or 256 views of 256 points each, with a 20, 30, or 45 cm field-of-view, depending on the resolution required. *Mx'* and *My'* were used to calculate the phase angle for each pixel with a signal amplitude above a preset threshold. The use of an amplitude threshold prevented phase calculation at pixels containing mostly noise (of which the phase is essentially random) or other very low intensity signal. This has the twin advantage of reducing calculation time and improving the appearance of the resulting phase map.

The problem of phase shifts introduced by field nonuniformities and chemical shift phenomena was overcome by running the sequence twice, once with the flow encoding modifications and once without. Subtraction of one phase map from the other resulted in cancellation of all phase shifts except those due to flow. Misregistration effects between the two scans were minimised by interleaving acquisitions, i.e., the first view of the second scan was acquired between the first and second views of the first scan, and so on.

The sequence was initialized by gating to the R-wave of the electrocardiogram, and a gating delay could be introduced before the first excitation pulse. The sequence was repeated up to 12 times every heartbeat at intervals of between 50 and 100 ms; this allowed phase maps to be produced giving flow information over part or all of the heart cycle as required. The technique was thus used to study blood flow in and around the heart. A comparison was also made of flow measurement in the femoral artery with Doppler ultrasound using a GEC/Picker Mobile Artery and Vein Imaging System at the Vascular Unit of the Medical Physics Department, Dulwich Hospital.

RESULTS

An image obtained by using the field even echo rephasing sequence is shown in Fig. 5. Very high

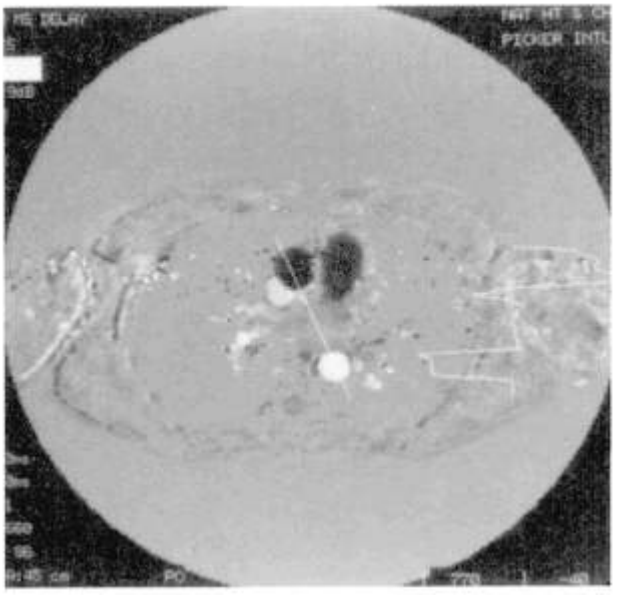

FIG. 7. The phase map for 170 ms delay with a flow profile drawn through the ascending and descending aorta. The velocity scale is calibrated in mm/s.

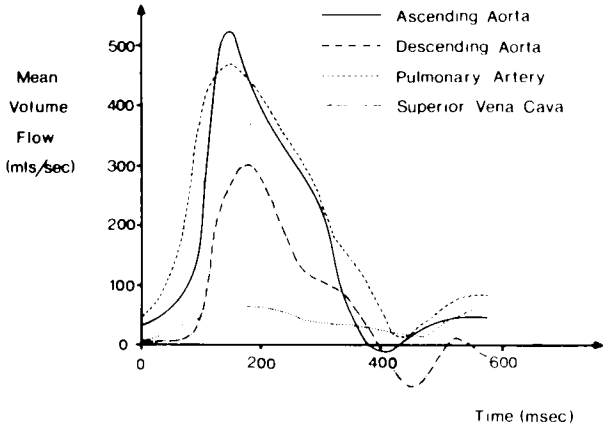

FIG. 8. A plot of mean volume flow (slice select direction) versus time, for the ascending aorta, descending aorta, pulmonary artery, and superior vena cava.

signal can be seen from all the principal blood in the selected slice, a transverse section through the left atrium. Twelve views of the slice were recorded during each heartbeat, resulting in phase maps at R-wave delays from 20 to 570 ms, in 50 ms intervals; the first nine of these are shown in Fig. 6. The gradient profiles used sensitised the image phase to flow in the slice select direction, i.e. along the longitudinal axis of the body; blood flowing up the body tends toward black and that flowing down the body towards white, stationary material appearing midgrey. High flow can be seen during systole in the ascending aorta, descending aorta, and pulmonary artery. Flow can also be seen in the superior vena cava throughout the heart cycle.

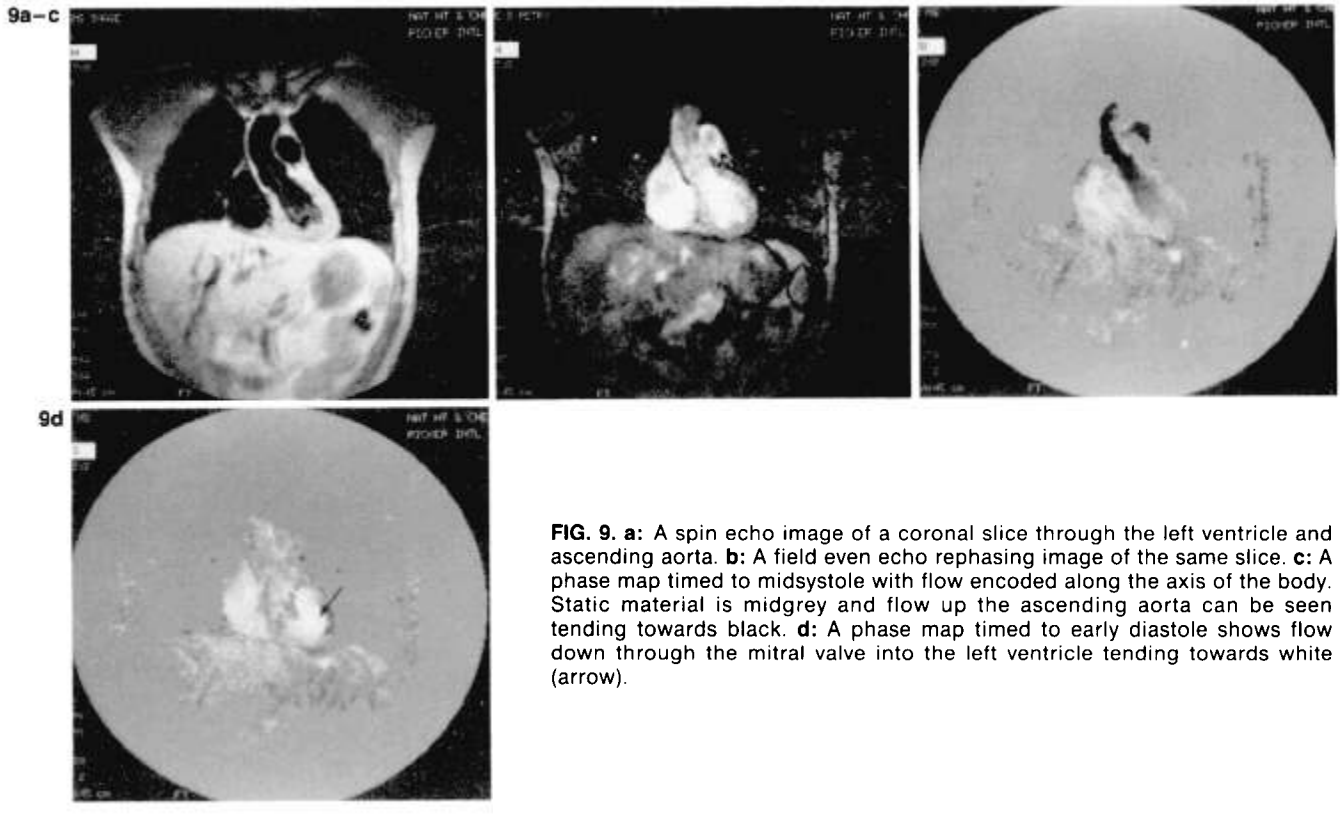

FIG. 9. a: A spin echo image of a coronal slice through the left ventricle and ascending aorta. **b:** A field even echo rephasing image of the same slice. **c:** A phase map timed to midsystole with flow encoded along the axis of the body. Static material is midgrey and flow up the ascending aorta can be seen tending towards black. **d:** A phase map timed to early diastole shows flow down through the mitral valve into the left ventricle tending towards white (arrow).

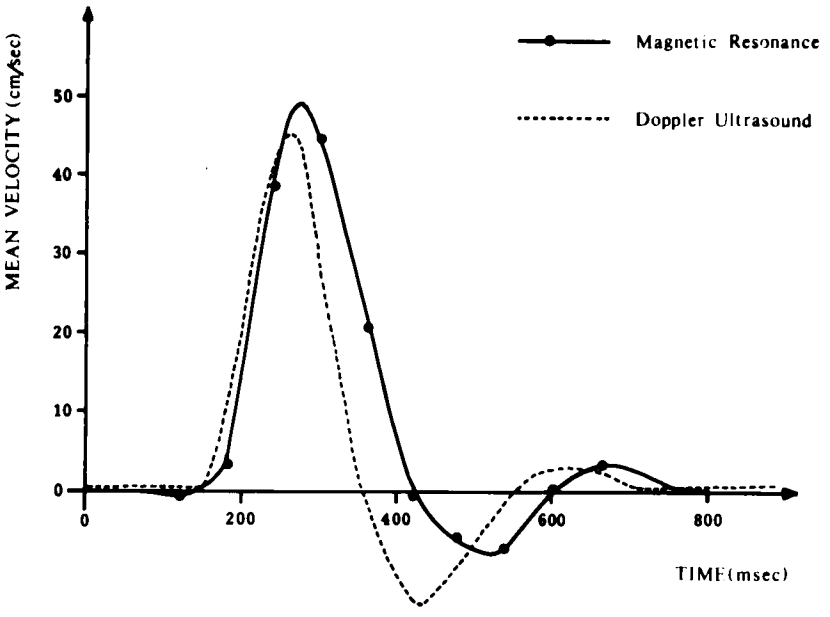

FIG. 10. A graph comparing MR and Doppler ultrasound for flow measurements in the femoral artery.

The technique is quantitative; Fig. 7 shows the phase map for the 170 ms delay with a flow profile drawn through the ascending and descending aorta, the velocity scale being calibrated in mm/s. Integration of flow velocities over the area of each vessel also results in mean volume flow rates; values for these are plotted against time for each of the four vessels concerned (Fig. 8). It should be noted that this is only the flow velocity component perpendicular to the imaging plane; to measure the total velocity of flow the sequence would have to be repeated twice more with gradient modifications to encode flow in the phase encode and read directions. In the case of the vessels considered here, however, the flow is predominantly in the slice select direction. Figure 9 shows an example of the use of the sequence with flow encoded in the read direction of a coronal slice through the left ventricle and ascending aorta. Only two of the phase maps are shown, one timed to midsystole showing high flow in the ascending aorta, and one timed to early diastole showing flow down into the left ventricle through the mitral valve.

Figure 10 shows a comparison of the technique with Doppler ultrasound, flow measurement in the femoral artery. It can be seen that the plots are very similar; any variations may be attributable to physiological factors, the examinations being made at different locations and times.

DISCUSSION

The technique described here overcomes problems that have previously obstructed the use of MR for routine measurement of blood flow. It allows for quantitative flow information to be obtained over the complete cardiac cycle within two scan times. Although the technique has previously been validated in vitro (11), in vivo accuracy has yet to be assessed. However, the technique observes only the phase of $Mx'y'$, which is largely independent of physiological factors and thus should not introduce significant errors. Such in vivo validation work is currently in progress. It is believed that the technique will be useful as a fast and accurate method of measuring flow which can be used alongside normal imaging to better assess a large proportion of cardiovascular disease.

Acknowledgment: We would like to thank the staff of the Magnetic Resonance Unit, National Heart and Chest Hospitals and Picker International for their helpful advice and discussions. The work was made possible by financial support from the Halley Stewart Trust (DNF), the Coronary Artery Disease Research Association, the Board of Governors of the National Heart and Chest Hospitals, and the League of Friends of the Brompton Hospital.

REFERENCES

1. Grant JP, Back C. NMR rheotomography: feasibility and clinical potential. *Med Phys* 1982;9:188–93.
2. Singer JR, Crooks LE. Nuclear magnetic resonance blood flow measurements in the human brain. *Science* 1983;221:654–6.
3. Axel L. Blood flow effects in magnetic resonance imaging. *AJR* 1984;143:1157–66.
4. Bryant DJ, Payne JA, Firmin DN, Longmore DB. Measurement of flow with NMR imaging using a gradient pulse and phase difference technique. *J Comput Assist Tomogr* 1984;8:588–93.
5. Feinberg DA, Crooks L, Hoenninger J, Arakawa M, Watts J. Pulsatile blood velocity in human arteries displayed by magnetic resonance imaging. *Radiology* 1984;153:177–80.

6. George CR, Jacobs G, MacIntyre WJ, et al. Magnetic resonance signal intensity patterns obtained from continuous and pulsatile flow models. *Radiology* 1984;151:421–8.
7. Mills CM, Brant-Zawadzki M, Crooks LE, et al. Nuclear magnetic resonance: principles of blood flow imaging. *AJR* 1984;142:165–70.
8. Redpath TW, Norris DG, Jones RA, Hutchison JM. A new method of NMR flow imaging [Letter]. *Phys Med Biol* 1984;29:891–5.
9. Van Dijk P. Direct cardiac NMR imaging of heart wall and blood flow velocity. *J Comput Assist Tomogr* 1984;8:429–36.
10. Moran PR, Moran RA, Karstaedt N. Verification and evaluation of internal flow and motion. True magnetic resonance imaging by the phase gradient modulation method. *Radiology* 1985;154:433–41.
11. Pattany PM, Nayler GL. High velocity flow imaging by even echo rephasing. [Abstract]. In: *Program of the Fourth Annual Meeting of the Society of Magnetic Resonance in Medicine*, London, August 19–23, 1985:599–600.
12. Packer KJ. The study of slow coherent molecular motion by pulsed nuclear magnetic resonance. *Mol Phys* 1969;17:355–68.
13. Waluch V, Bradley WG. NMR even echo rephasing in slow laminar flow. *J Comput Assist Tomogr* 1984;8:594–8.
14. Carr HY, Purcell EM. Effects of diffusion on free precession in nuclear magnetic resonance experiments. *Phys Rev* 1954;94:630–8.
15. Moran PR. A flow velocity zeugmatographic interlace for NMR imaging in humans. *Magn Reson Imaging* 1982;1:197–203.